

LETTER

Experimental partitioning of Sr and Ba in Kiglapait feldspars† ‡

S.A. MORSE^{1,*} AND JULIEN ALLAZ²

¹Department of Geosciences, University of Massachusetts, 611 North Pleasant Street, Amherst, Massachusetts 01003-9297, U.S.A.

²Department of Geological Sciences, University of Colorado, UCB 399, Boulder, Colorado 80309-0399, U.S.A.

ABSTRACT

New electron microprobe analyses of Sr and Ba in feldspars and coexisting experimental glasses show very strong correlations of the partition coefficients with the ternary Or content of the feldspar. The correlations therefore scale inversely with temperature, as also found in the literature. The Sr content of feldspars is maximized in mesoperthite and decreases with evolution of feldspar to the ternary minimum. The relationship of $D_{Sr/L}$ to decreasing X_{An} is initially flat at a value of 1.8 but curves sharply upward past 6.5 after the arrival of apatite at An_{38} . A similar concave-up curve at much higher values of D is found in the literature. The value of D (nine points) scales linearly with ternary Or; $R^2 = 0.99$. Experimental feldspars are consistently richer in Sr than natural ones at comparable An. They jump from 200 ppm higher to 400 ppm higher at Ap^+ . Experimental glass compositions are correspondingly low in Sr, so the material balance is conserved. Inversion of natural feldspars to liquid compositions using the experimental partition coefficients fails because the experimental crystals contain enhanced values of Sr from the apatite and feldspar components of the melted rock compositions. The partitioning of Ba (five points; range 0.4 to 6.1) also scales with ternary Or; $R^2 > 0.99$; and there is no systematic difference between the natural and experimental concentrations of Ba in the feldspars. The inversion of D to liquid compositions may be safe for Ba but must be approached with caution for Sr.

Keywords: Element partitioning, strontium, barium, Kiglapait, experimental, analytical, Sr and Ba in feldspar

INTRODUCTION

The role of strontium in feldspars is confusing and unclear when samples from various bulk compositions are considered (Smith and Brown 1988, esp. p. 362–365). One thing certain is that on the whole, the partitioning of Sr into feldspars follows a concave-upward curve in plagioclase from An_{100} to about An_{30} (ibid, Fig. 14.24). Drake and Weill (1975) found that partition coefficients for Sr were always greater than unity but for Ba less than unity at high temperatures, with both strongly dependent on temperature. Morse (1982) found a decrease of $D_{Sr/L}$ with the arrival of apatite and a preference for Sr in monoclinic sanidines compared to triclinic plagioclase. Blundy and Wood (1991) examined a wealth of literature data and showed a strong correlation between D_{Sr} (and D_{Ba}) with plagioclase composition and developed a lattice strain model to show the preference for both these elements in more sodic plagioclase. In an experimental study of hydrous metapelites, Icenhower and London (1996) found the partitioning of Sr to be independent of either the albite or the orthoclase component of the plagioclase, whereas they found a strong correlation with orthoclase for Ba and Rb. In another hydrous study using alkali feldspars, Henderson and Pierozynski (2012) showed a strong correlation for both Sr and Ba with the increasing Or content of the melt, among other compositional features.

Here we use new analyses of melting experiments at 5 kbar with temperatures ranging from 1250 to 1020 °C using finely ground mixtures and rock samples from the Kiglapait intrusion, Labrador (Morse et al. 2004). We show strong correlations of both Sr and Ba partitioning with Or.

In the Kiglapait stratigraphic progression the feldspars run around the Ab-rich corner of the ternary as antiperthites and mesoperthites, then continue an enrichment in Or until they reach a ternary minimum composition at about $Or_{33}An_{10}Ab_{57}$ (Supplementary Fig. 1¹). These evolved compositions are consistent with ternary feldspar models at high temperature and moderate pressures (Fuhrman and Lindsley 1988). Here the textures are highly variable (Morse 1969, plates 47–49), ranging from oligoclase embayed by K-feldspar to coarser wormy intergrowths unmixed from hypersolvus feldspar. The mesoperthites are partially unmixed from a monoclinic Na-sanidine (Speer and Ribbe 1973), also called Ca-sanidine in some classifications.

Analysis of the data shows that the Sr concentration in feldspar scales with ternary Ab (Fig. 1). The peak Sr concentration at 797 ppm is reached in a mesoperthite sample KI 4061, 99.94 PCS (volume percent solidified) $An_{17.7}Ab_{67.5}Or_{14.8}$. The locus of the high-Sr compositions is nearly constant at about 67.5% ternary Ab. There is a composition discriminant at 600 ppm Sr. Below that value the mineral is plagioclase with Sr near 500 ppm.

* E-mail: tm@geo.umass.edu

† ‡ Open access: Article available to all readers via GSW (<http://ammin.geoscienceworld.org>) and the MSA web site.

¹ Deposit item AM-13-1113, Figure and Table. Deposit items are stored on the MSA web site and available via the *American Mineralogist* Table of Contents. Find the article in the table of contents at GSW (ammin.geoscienceworld.org) or MSA (www.minsocam.org), and then click on the deposit link.

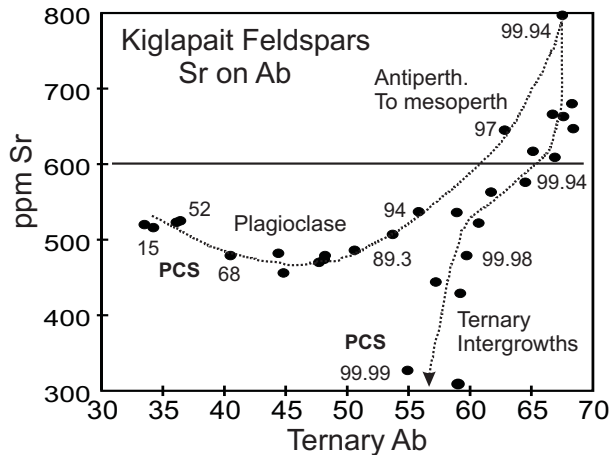


FIGURE 1. Concentration of Sr in Kiglapait feldspars from 15 to 99.99 PCS in the intrusion (where PCS = volume percent solidified). Data from Table 1 of Morse (1982), with PCS values as a guide to stratigraphic height. The highest concentration occurs in mesoperthite, followed by a decreasing trend as the feldspars approach and reach the ternary minimum at lower concentrations of Ab.

Above 600 ppm the crystals are antiperthite to mesoperthite, and as they follow a continuing path of falling Ab and Sr but increasing Or, the crystals are ternary intergrowths.

Elements of particular interest in this discussion have nominal abundances in the Kiglapait intrusion estimated at 0.22% K_2O (Morse 1981), 532 ppm Sr (Morse 1982), and ~74 ppm Ba. The value for Ba is obtained from an extrapolated array of feldspar analyses (Morse, in preparation) yielding 110 ppm Ba in the earliest feldspars, which amount to 67% of the mass of the intrusion (Morse 1979, 1981).

EXPERIMENTAL METHODS

Trace element partitioning

An ongoing project to retrieve element partitioning data from the experimental results of Morse et al. (2004) utilizes the high precision available with the two Cameca electron microprobes at the University of Massachusetts-Amherst. Major element chemistry in glass and feldspars was first determined on a Cameca SX-50. These results were then utilized as fixed compositions to measure trace amounts of Sr and Ba in the same material. Standards used were $BaSO_4$ and SrF_2 . Analysis conditions for trace element analyses were 15 kV, 100 nA, and 10 μm beam in all materials, to maximize the analytical precision and minimize the diffusion effect. Peak counting time on each spectrometer and for each element was varied between 60, 200, and 400 s in all samples. Results were identical independent of the variable counting time, which ensured that diffusion has not affected the results. Thus, final results reported in Table 1 were obtained by averaging all analyses ($n = 17$ to 40), yielding a standard deviation of 14 to 29 ppm for Sr and 18 and 39

ppm for Ba. Background counting time was identical to the peak counting time. Sr was first analyzed, aggregating the intensities of two large and two very large PET crystals. Only a single background on the high side of the $SrL\alpha$ peak was selected, with a fixed slope of 0 constrained by a WDS scan, as the low side is affected by the Si absorption edge ($SiAK$). Similar analytical conditions were applied for a second analysis including $BaL\alpha$ on two LPET crystals and $TiK\alpha$ on one LiF crystal. A two-point exponential background was used on $BaL\alpha$; the curvature of the exponential was constrained by a WDS scan. Ba analyses were corrected for interference from $TiK\alpha$ on PET.

Detection limits for both feldspars and glass were ~18 ppm for Sr using 200 s counting time and ~34 ppm for Ba at 100 s counting time. The low detection limit for Sr is a function of the long counting time and high beam current: for 60 s counting time the detection limit for Sr is only ~46 ppm.

Strontium

The results for Sr are shown in Table 1 and in Figures 1 to 4. Natural feldspar compositions (Fig. 1) range from ~500 ppm Sr in the Lower Zone (0–84 PCS) and early Upper Zone to 94 PCS where apatite arrives in the rock sequence. Then the Sr content rises sharply to 797 ppm where the feldspars are antiperthites to mesoperthites, then drops sharply as the feldspars become complex ternary intergrowths.

Experimental plagioclase compositions range from a minimum of 673 ppm Sr to a maximum of 1074 ppm; the glass compositions run from 103–434 ppm.

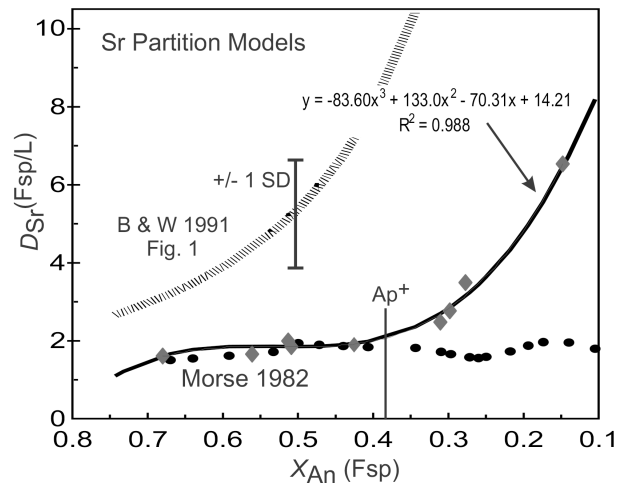


FIGURE 2. Models for the partitioning of Sr in feldspar. Filled ovals: as estimated from XRF compositions using liquids calculated by summation over the rocks of the Kiglapait intrusion (Morse 1982). Solid curve with gray diamond data points: this study, Table 1; from melting experiments in graphite on Kiglapait bulk compositions at 5 kbar (Morse et al. 2004). Shaded curve: from Figure 1 of Blundy and Wood (1991), taken as a power-law regression through the scattered array of ~127 data points with $X_{An} > 0$. The experimental curve for the sodic feldspars takes a form similar to the Blundy and Wood data. Ap^+ signifies the arrival of cumulus fluorapatite at 94 PCS.

TABLE 1. Sr and Ba experimental data for Kiglapait feldspars and glass, 5 kbar graphite

KI Sp/No	Sample Exper*	Gl %	X_{An} Fsp	X_{An} Glass	T^* °C	Sr Fsp ppm	Sr Gl ppm	$D(Sr)$ Fsp/Gl	Or Fsp norm %	Ba Fsp ppm	Ba Gl ppm	$D(Ba)$ Fsp/Gl
na	KI-1-1	70	0.678	0.549	1253	711	434	1.64	0.6			
na	KI-39-1	89	0.559	0.366	1204	673	398	1.69	0.6			
na	2K-14-2	40	0.512	0.343	1202	734	361	2.04	0.6			
na	2K-14-3	71	0.507	0.32	1203	707	373	1.90	0.3			
na	2K-14-1	62	0.424	0.324	1100	678	354	1.91	2.2	34	98	0.35
4079	KU-44-2	90	0.308	0.164	1060	872	352	2.48	7.2	2704	3355	0.81
4083	KU-35-1	97	0.297	0.2	1046	948	342	2.77	10.5	5558	4481	1.24
3381	KU-44-1	90	0.275	0.169	1035	1074	306	3.51	15.4	10649	5437	1.96
4077	KU-35-3	99	0.145	0.175	1019	675	103	6.53	47.8	20060	3310	6.06

Notes: KI 4077 Ba data from Peterson (1999); see Supplement. EMPA data in bold type.

* Morse et al. (2004); T smoothed on An .

As shown in Figure 2, the experimental partition coefficient for Sr in plagioclase is almost constant near 1.8 until the plagioclase composition reaches An_{38} , then climbs strongly to a value of 6.5 at An_{15} .

At this high value of D_{Sr} , the feldspar KI 4077 is a sanidine with ternary $X_{Or} = 47.8$ (Table 1 and Supplementary Table 1¹) and ternary $X_{Or} = 7$; it lies at the upper An limit in Supplementary Figure 1¹ at $X_{An} \sim 0.54$. It coexists with liquid $Or_{31}Ab_{57}An_{12}$ (Supplementary Table 1¹) that plots among the most potassic group of wet chemical analyses in Supplementary Figure 1¹.

The curve in Figure 2 is shown compared to the estimates of Morse (1982) from summation. The old estimates are essentially the same as the new experimental ones from high values of An down to the plagioclase composition An_{38} where Ap^+ occurs at 94 PCS. Thereafter the Sr abundance in the summation liquid differs strongly, as discussed below. Also shown in Figure 2 is the trend of many literature estimates by Blundy and Wood (1991) that, although it plots at values considerably higher than found here, also shows a strong concave-up trend. The scales of the two studies are not wholly comparable because of the long troctolitic history of the Kiglapait LZ, tending to stretch out the flat part of the experimental curve.

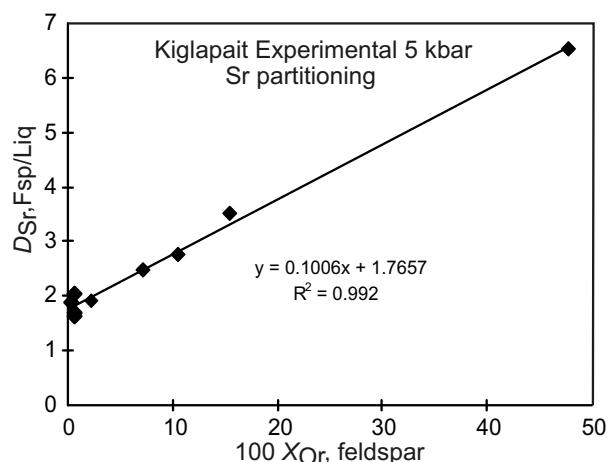


FIGURE 3. Experimental partitioning results (Table 1) for Sr plotted against ternary Or. The intercept at $D = 1.8$ comports with the estimates in Figure 2 for $X_{An} > 0.34$, which marks the arrival of apatite (Ap^+).

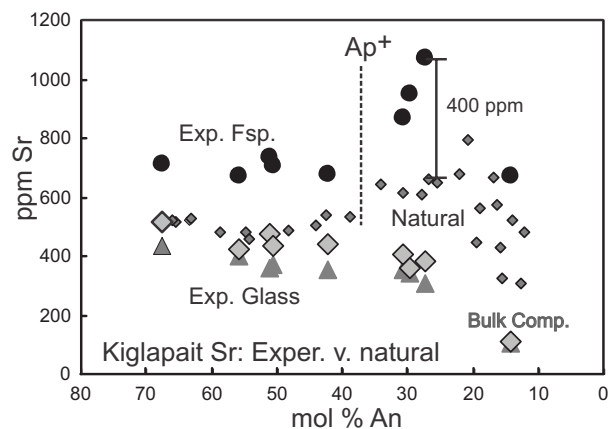


FIGURE 4. Sr contents of experimental (Exp.) and natural Kiglapait feldspars. The experimental feldspars have approximately 200 ppm more Sr at high An (Lower Zone samples) and up to 400 ppm more after the arrival of apatite (Ap^+). The experimental glass compositions are shown as large gray triangles, illustrating that the material balance of Sr is nominally conserved; the large gray diamond symbols show the nominal bulk compositions calculated from the experimental feldspar and glass compositions. The experimental feldspars have evidently scavenged Sr from the feldspar and apatite components of the melt.

The experimental partition coefficient for Sr in feldspar is strongly correlated with the Or content of the feldspar, as shown in Figure 3. This is not surprising, given the large K site into which Sr (and Ba) can enter with little strain, but the strength of the correlation is remarkable. The coupled substitution is readily understood as charge-balanced $SrAl(KSi)_{-1}$.

DISCUSSION OF THE DIVERGENCE BETWEEN SUMMATION AND PARTITIONING

If the experimental determination of Figure 2 is used to calculate the liquid composition from the observed natural feldspars (Morse 1982), the liquid shows a steep downward trend from ~ 280 ppm near 94 PCS to 50 ppm at the end of crystallization. In contrast, the summation liquid has 245 ppm at 99.98 PCS (Morse 1982, Table 4). The depletion trend required by the experimental result is impossible: the process of summation begins at the top of the intrusion and works its way downward. It is therefore most secure at the highest stratigraphic levels. The final liquid at the ternary minimum feldspar composition has no Mg left and nowhere else to go. Its crystallized form therefore has the liquid composition. The summation process requires that the true liquid follow closely the trend of the rocks, which declines slowly from 430 ppm at 99.75 PCS to 278 ppm at 99.98 PCS (Morse 1982, Fig. 2 therein).

The alternative choice is to consider the possibility that the experimental feldspar crystals contain more Sr than the corresponding natural ones, and that is decidedly the case, as shown in Figure 4. Moreover, the difference is about 200 ppm before Ap^+ , but jumps to about 400 ppm after that. Correspondingly, the experimental glass compositions are much lower in Sr than the natural feldspar compositions (Fig. 4), so the material balance is nominally conserved. The amount of glass in the experiments (Table 1) averages 79%. The amounts of feldspar vary from 1 to 40%, but in the group with $An < 38$ the glass amounts are 10, 3, 10, and 1%, respectively. Accordingly, the experimental feldspars have scavenged the majority of Sr present in the natural feldspar and apatite components of the melted rocks, leaving modest amounts in the experimental glasses.

Because of this enhancement of Sr in the experimental feldspars, the partition coefficients cannot be used directly to infer the natural liquid compositions by inversion.

BARIUM

Wet chemical analyses of feldspars (Morse, in preparation) show high values of BaO ranging from ~ 1.0 to 1.4 wt% in very evolved feldspar compositions. The content of Ba is inversely related to the An content of the feldspar. Although experimentally grown K-rich feldspars were observed up to 2.2% BaO by Peterson (1999; Supplementary Table 1¹ here), there is no systematic difference between the experimental and natural Ba contents of the four feldspar compositions studied. Our data show partitioning results for five bulk compositions summarized in Table 1 here and illustrated in Figure 5. The charge-balanced relationship of Ba to K is given by the coupled exchange reaction $BaAl(KSi)_{-1}$ and is expected because the large ionic radius of Ba^{2+} (1.35 Å) is compatible with that of K^+ (1.38 Å). We find (Fig. 5) that the value of the partition coefficient D is linear against the Or content of the feldspar with a vanishingly small error. Although expected in principle, the degree of correlation is astounding.

The presence of significant Ba in highly evolved feldspars

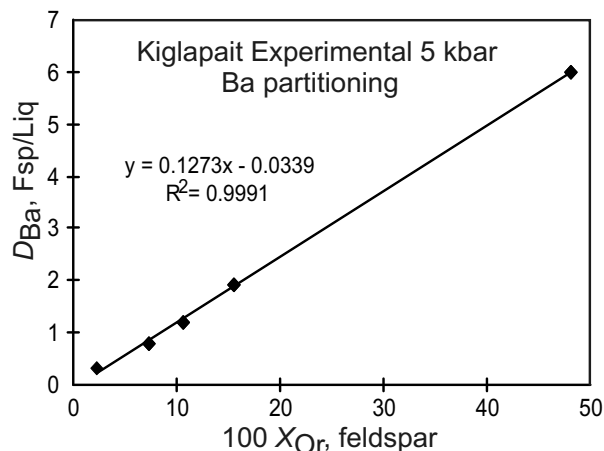


FIGURE 5. Ba partitioning plotted from the data in Table 1.

and liquids has an effect on the formal investigation of feldspar-liquid linear partitioning (e.g., Morse et al. 2004, Fig. 16). The crystal composition presents no problem, because the An content is determined solely from the Ca content. The An composition of the liquid, however, is normally calculated from the residual Al after Ab and Or are formed (e.g., Morse 2013b). If Ba is present in significant quantity, then that element must be allotted a corresponding amount of Al to make celsian, CN, $\text{BaAl}_2\text{Si}_2\text{O}_8$. When this is done, the residue given to An is less than before (so the proportion of Ab is greater) and hence the partition coefficient $X_{\text{Ab}}^{\text{S}}/X_{\text{Ab}}^{\text{L}}$ decreases from that in a low-Ba system. To correct for this effect, a conventional oxygen-norm program with a CN option was used to calculate the liquid composition for the last four samples in Table 9 of Morse et al. (2004), giving a corrected linear partitioning diagram. As expected, the intercept now falls slightly below 1.0 and the K_D value rises slightly, from 0.524 to 0.541.

IMPLICATIONS

Both the positive correlations of Sr and Ba with Or occur negatively correlated with temperature, as explicitly found by Henderson and Pirozynski (2012) for alkali feldspars. They are potentially useful in recovering the compositions of liquids in the troctolite-norite and related mafic suites of rocks.

The evolution of the Kiglapait magma after a long history of making troctolite and olivine gabbro resulted in terminal feldspar compositions at the extreme compositional limit, the ternary minimum. Despite their initially low concentrations listed above, the excluded elements K and Ba have increased by factors of ~14 and 118, respectively. This evolution stands in contrast to

the Skaergaard intrusion, where the evolution stops at oligoclase, probably because it has more trapped liquid for which $D = 1.0$ for all components (Morse 2013a). Despite being depleted overall by a factor of ~0.4 in the rocks from base to top, Sr has attained a high concentration in Kiglapait mesoperthite and both it and Ba are enriched with the Or component of feldspar. These anhydrous experimental results are in accord with those found in hydrothermal experiments by Henderson and Pirozynski (2012).

ACKNOWLEDGMENTS

The support of the electron instrumental facilities at the University of Massachusetts under the leadership of Michael Jercinovic has been central to the success of these studies. The thesis work of Abigail Peterson is gratefully acknowledged here. J.A. was supported during this study by a post-doctoral fellowship under the direction of Michael Williams and Michael Jercinovic supported by the Electron Microprobe Facility in the Department of Geosciences at the University of Massachusetts. This article is based on research supported by NSF under Award No. EAR-9526262 to Williams and -0948095 to Morse.

REFERENCES CITED

- Blundy, J.D., and Wood, B.J. (1991) Crystal-chemical controls on the partitioning of Sr and Ba between plagioclase feldspar, silicate, melts, and hydrothermal solutions. *Geochimica et Cosmochimica Acta*, 55, 193–209.
- Drake, M.J., and Weill, D.F. (1975) Partition of Sr, Ba, Ca, Y, Eu^{2+} , Eu^{3+} , and other REE between plagioclase feldspar and magmatic liquid: an experimental study. *Geochimica et Cosmochimica Acta*, 39, 689–712.
- Fuhrman, M.L., and Lindsley, D.H. (1988) Ternary feldspar modeling and thermometry. *American Mineralogist*, 73, 201–215.
- Henderson, C.M.B., and Pirozynski, W.J. (2012) An experimental study of Sr, Ba, and Rb partitioning between alkali feldspar and silicate liquid in the system nepheline–kalsilite–quartz at 0.1 GPa $P(\text{H}_2\text{O})$: a revisit and assessment. *Mineralogical Magazine*, 76, 157–190.
- Icenhower, J., and London, D. (1996) Experimental partitioning of Rb, Cs, Sr, and Ba between alkali feldspar and peraluminous melt. *American Mineralogist*, 81, 719–734.
- Morse, S.A. (1969) The Kiglapait Layered Intrusion, Labrador. *Geological Society of America Memoir* 112, 204 pp.
- (1979) Kiglapait geochemistry II: Petrography. *Journal of Petrology*, 20, 591–624.
- (1981) Kiglapait geochemistry III: Potassium and rubidium. *Geochimica et Cosmochimica Acta*, 45, 163–180.
- (1982) Kiglapait geochemistry V: Strontium. *Geochimica et Cosmochimica Acta*, 46, 223–234.
- (2013a) Solidification of trapped liquid in rocks and crystals. *American Mineralogist*, 98, 888–896.
- (2013b) Experimental equilibrium tested by plagioclase loop widths. *Journal of Petrology*, 54, 1793–1813, DOI: 10.1093/petrology/egt031.
- Morse, S.A., Brady, J.B., and Sporleder, B.A. (2004) Experimental petrology of the Kiglapait intrusion: Cotectic trace for the Lower Zone at 5 kb in graphite. *Journal of Petrology*, 45, 2225–2259.
- Peterson, A.L. (1999) Quest for the liquid line of descent of the Upper Zone of the Kiglapait intrusion, Labrador, Canada: an experimental study, 80 pp. MS thesis, University of Massachusetts, Amherst.
- Smith, J.V., and Brown, W.L. (1988) *Feldspar Minerals*. Springer-Verlag, Heidelberg.
- Speer, J.A., and Ribbe P.H. (1973) The feldspars of the Kiglapait intrusion, Labrador. *American Journal of Science*, 273-A, 468–478.

MANUSCRIPT RECEIVED JUNE 6, 2013

MANUSCRIPT ACCEPTED AUGUST 29, 2013

MANUSCRIPT HANDLED BY IAN SWAINSON